Supplement of Ocean Sci., 16, 1459–1474, 2020
https://doi.org/10.5194/os-16-1459-2020-supplement

Ocean Science Open Access EGU

Supplement of

Seasonal variability of the Arabian Sea intermediate circulation and its impact on seasonal changes of the upper oxygen minimum zone

Henrike Schmidt et al.

Correspondence to: Henrike Schmidt (hschmidt@geomar.de)

The basic relation

$$\frac{d}{dt}(d\underline{L}) = \boldsymbol{D} \cdot d\underline{L}, \tag{1}$$

with $d\underline{L}$ the distance $(dx, dy) = (x_B - x_A, y_B - y_A)$ of two infinitesimal separated points A and B, and **D** the 'deformation matrix'

$$\boldsymbol{D} = \begin{pmatrix} \frac{\partial u}{\partial x} & \frac{\partial u}{\partial y} \\ \frac{\partial v}{\partial x} & \frac{\partial v}{\partial y} \end{pmatrix}, \tag{2}$$

describes the continuous deformation of $d\underline{L}$ by the velocity vector $\underline{u} = (u, v)$ at that position. Equation (1) originates directly from $d\underline{x} = \underline{u} \cdot dt$ and may be found in most treatises about hydrodynamics, e.g. Lamb (1879).

Lamb, S. H.: Hydrodynamics. University Press, Cambridge, 1879.

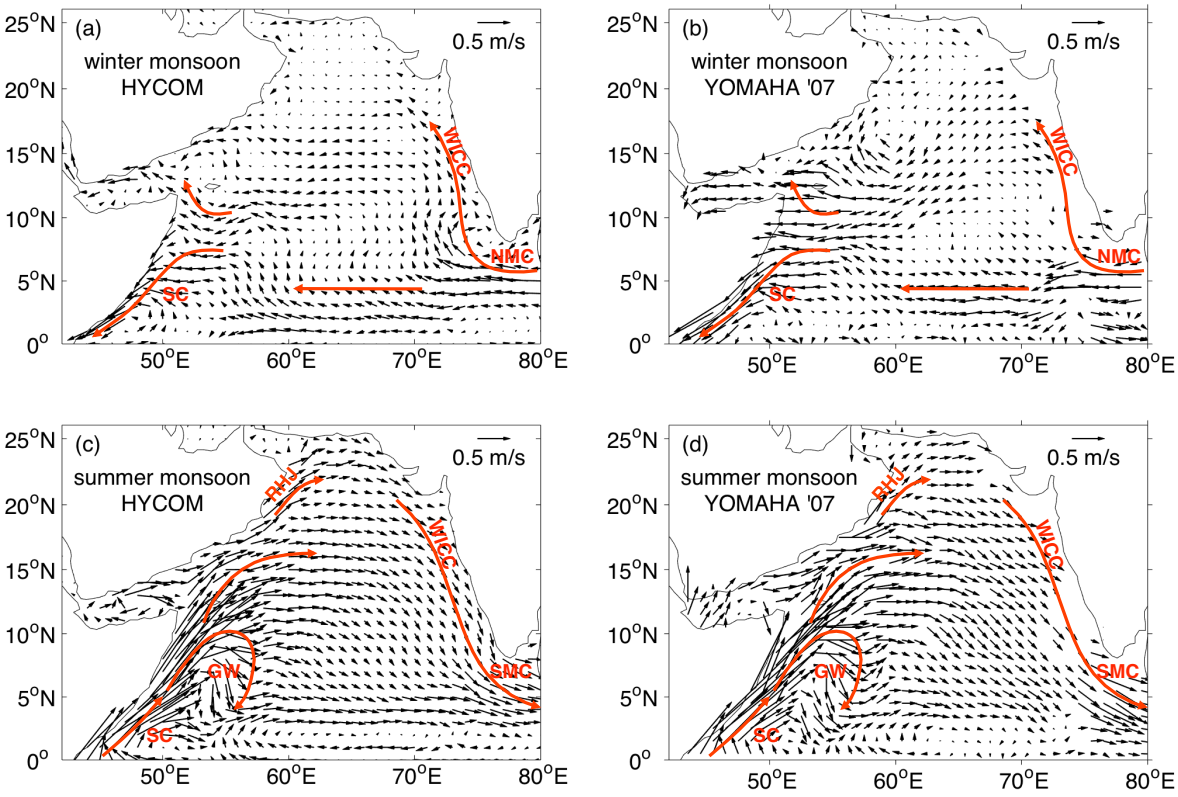

Figure S1: Mean surface velocity obtained from HYCOM (a, c) and YoMaHa'07 (b, d) between 1997 - 2007. Current branches indicated after Schott et al. (2009) are the Somali Current (SC), Northeast and Southwest Monsoon Current (NMC and SMC), Ras al Hadd Jet (RHJ), West Indian Coast Current (WICC) and Great Whirl (GW) for the winter monsoon (a, b) from November to February and the summer monsoon (c, d) from June to September.

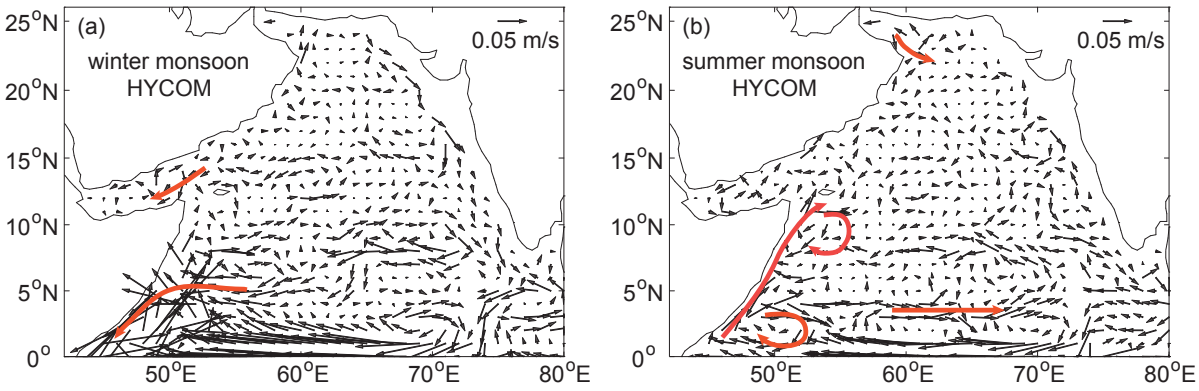

Figure S2: Mean velocity in 1000 m depth obtained from HYCOM between 2002 – 2007 for the winter monsoon (a) from November to February and the summer monsoon (b) from June to September. Current branches indicated after Vitale et al. (2017).

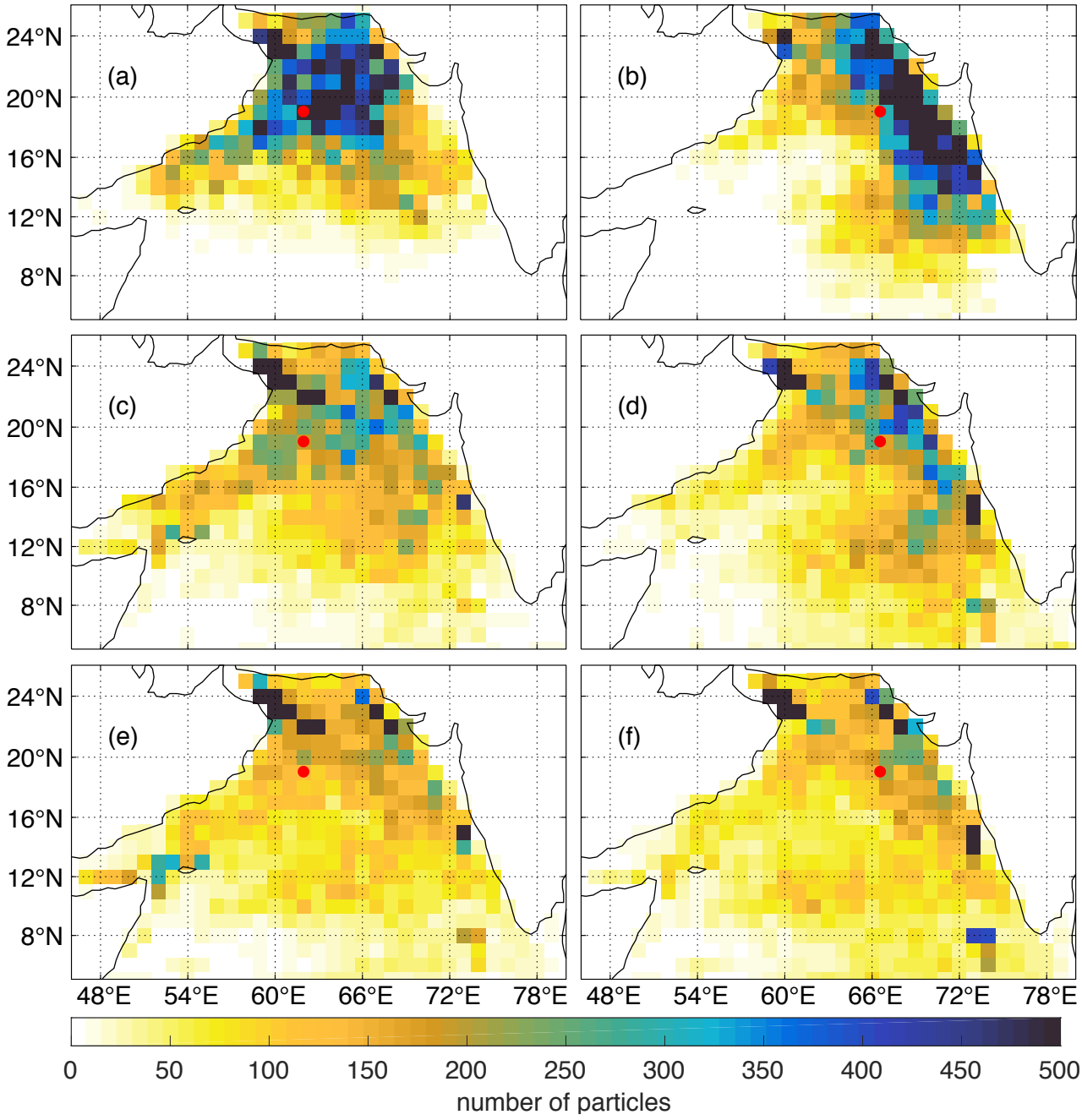

Figure S3: Lagrangian particle distribution after 4 (a, b), 8 (c, d) and 12 (e, f) years simulation for the WR (left) and the ER (right). Eastern (ER) and western (WR) release locations are marked in red.

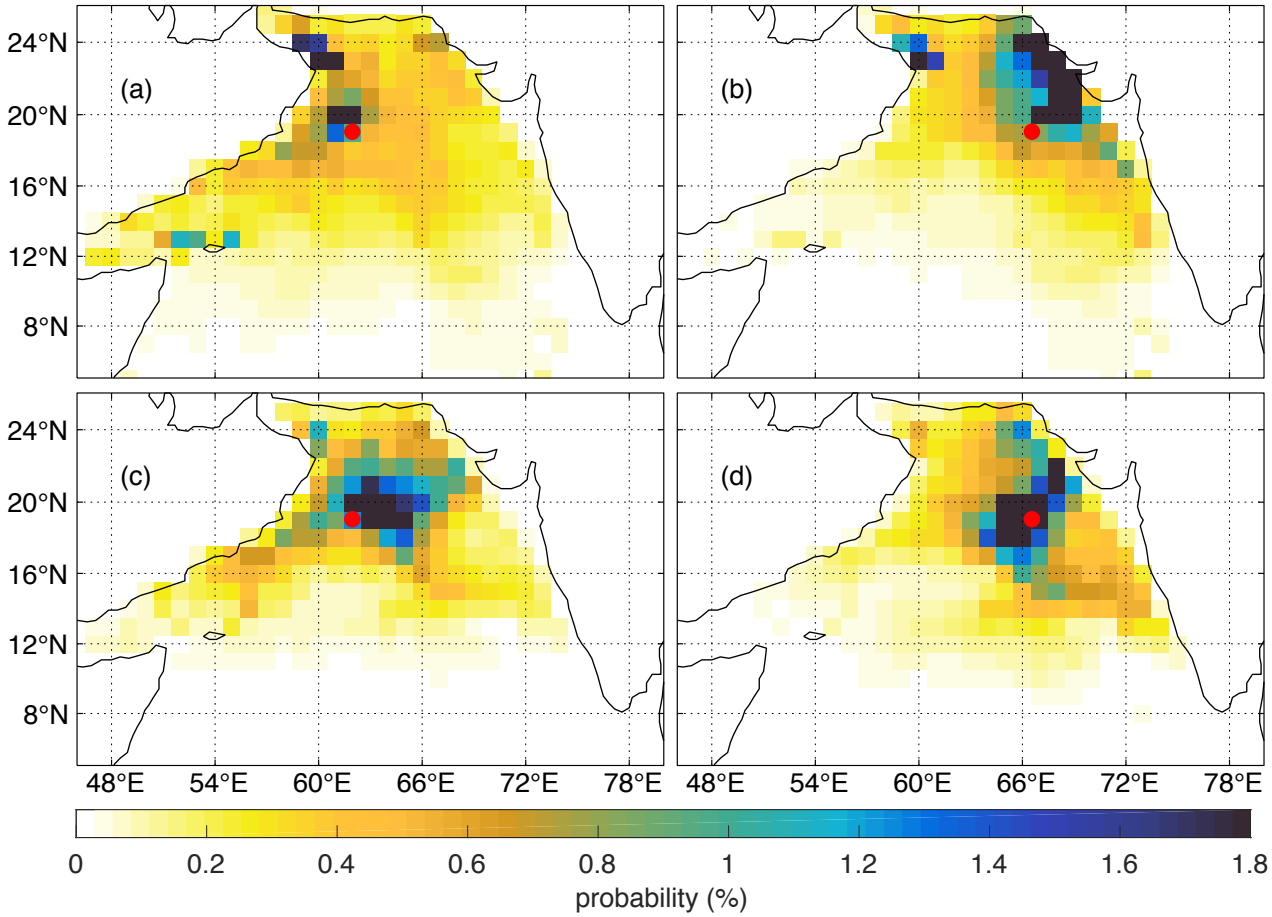

Figure S4: Same as Fig. 7 but for the density layers of σ=26.4 kg/m^3 (a, b) and σ=27.4 kg/m^3 (c, d).

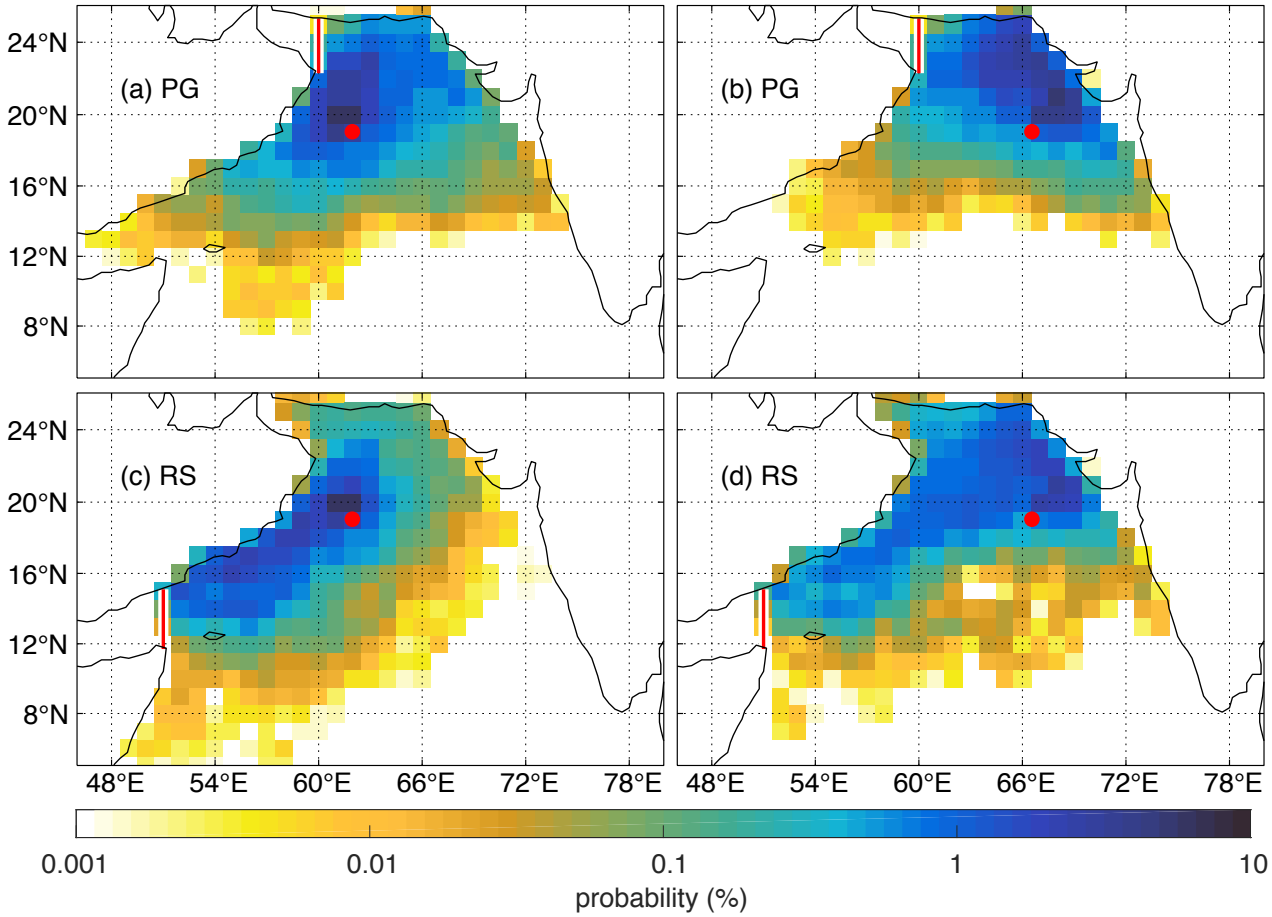

Figure S5: Same as Fig. 8 but for the density layer of σ=26.4 kg/m^3.

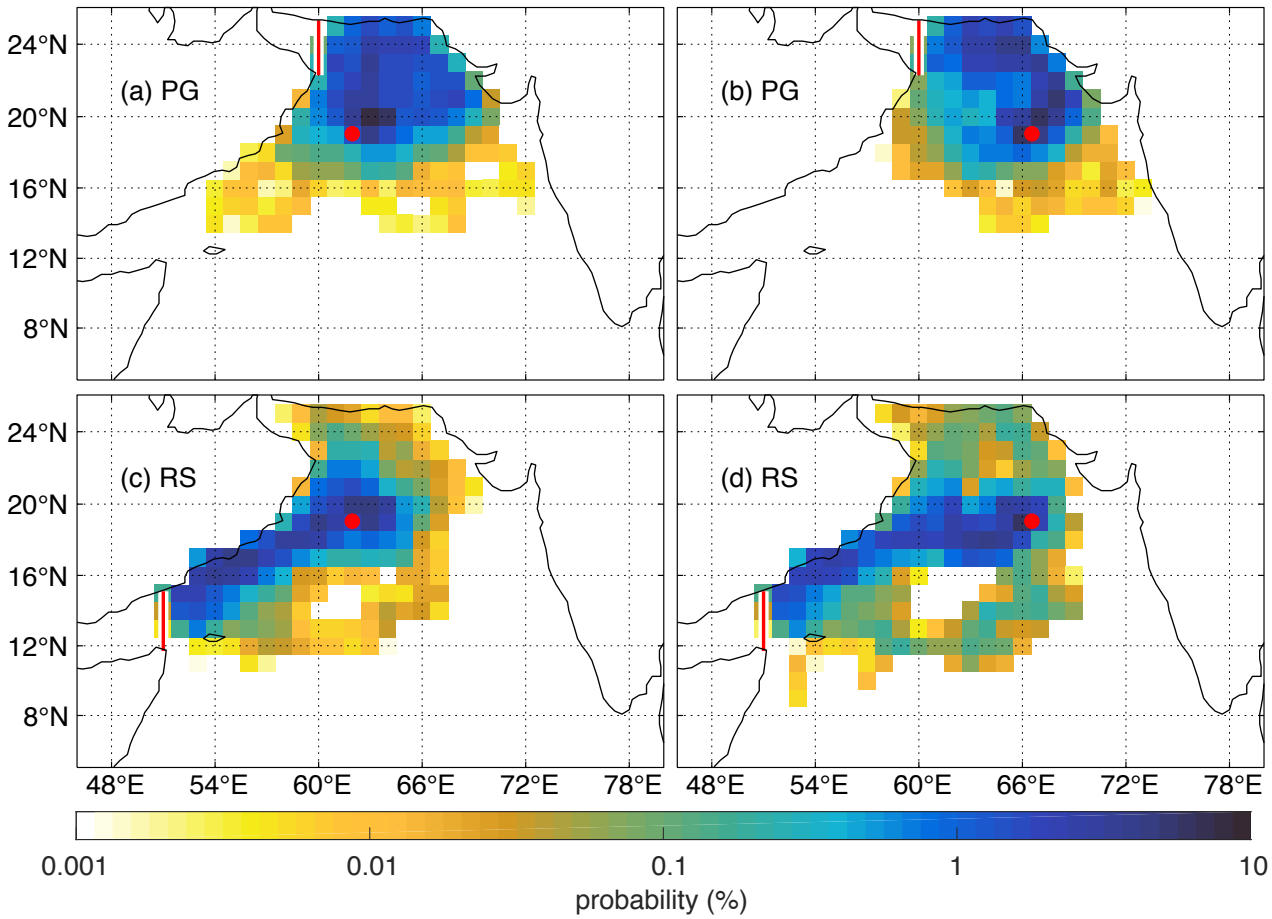

Figure S6: Same as Fig. 8 but for the density layer of σ=27.4 kg/m^3.

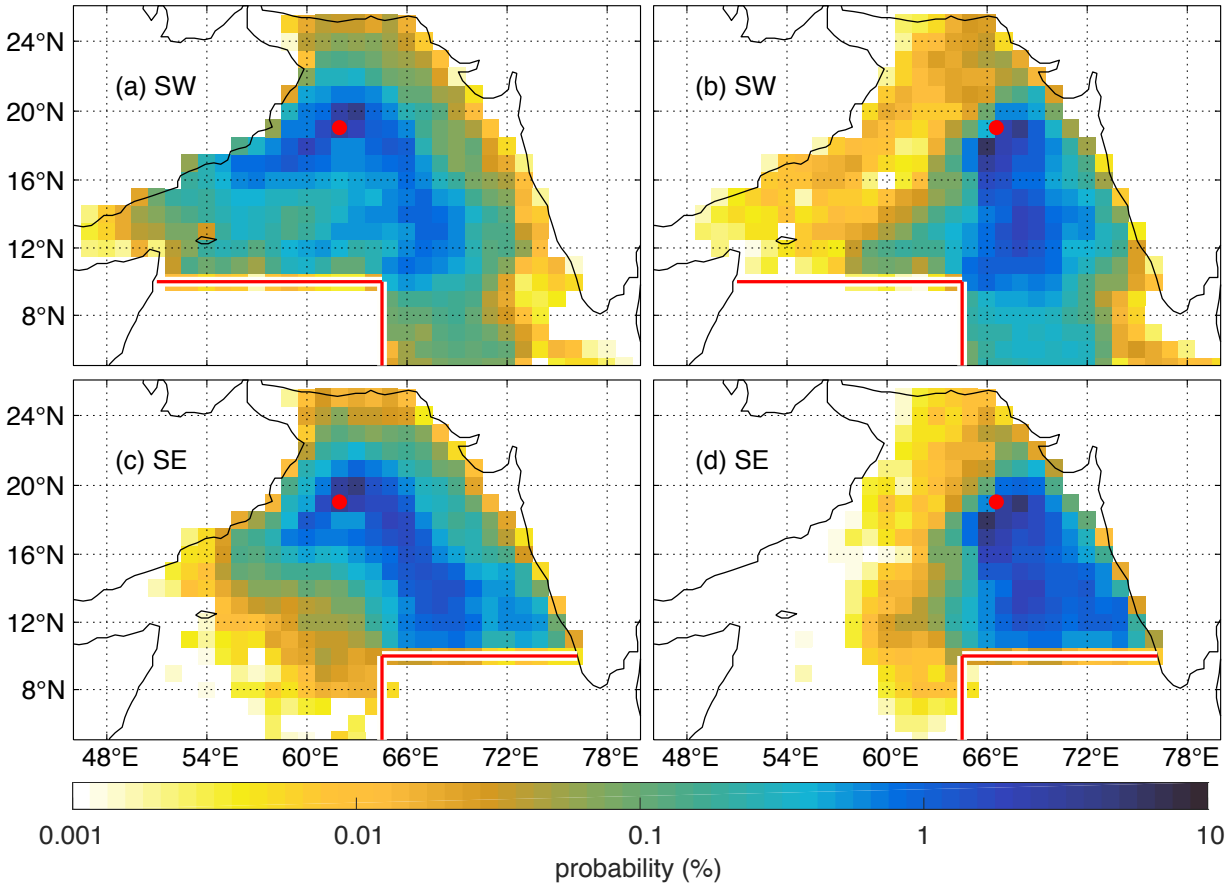

Figure S7: Lagrangian particle position probability maps show the most pronounced pathways of fluid particles along the isopycnal σ=27 kg m^{-3} for the backward trajectory analysis, entering the Arabian Sea from the south west (a, b) and the south east (c, d) streaming into the eastern (right) and western (left) basin. Eastern (ER) and western (WR) release locations in the OMZ are marked in red, as well as the sections, that need to be crossed, to define the source regions.